Sensors and Actuators B 181 (2013) 395–401

Contents lists available at SciVerse ScienceDirect

Sensors and Actuators B: Chemical

journal homepage: www.elsevier.com/locate/snb

Room temperature responses of visible-light illuminated WO_3 sensors to NO_2 in sub-ppm range

Chao Zhang[a,*], Abdelhamid Boudiba[a], Patrizia De Marco[b], Rony Snyders[b,c], Marie-Georges Olivier[a,c], Marc Debliquy[a]

[a] Service de Science des Matériaux, Faculté Polytechnique, University of Mons, Mons, Belgium
[b] Chimie des Interactions Plasma-Surfaces, CIRMAP, University of Mons, Mons, Belgium
[c] Materia Nova Research Center, Mons, Belgium

ARTICLE INFO

Article history:
Received 17 August 2012
Received in revised form 22 January 2013
Accepted 29 January 2013
Available online 7 February 2013

Keywords:
Tungsten oxide
Gas sensors
Nitrogen dioxide
Visible-light illumination
Room temperature

ABSTRACT

In this paper, the effects of visible-light illumination on sensing properties of tungsten trioxide (WO_3) sensors have been investigated. WO_3 sensitive films are prepared on alumina substrates by screen-printing. WO_3 sensors illuminated by visible/ultra-violet lights are submitted to sensing tests with 160 and 320 ppb nitrogen dioxide (NO_2) at room temperature. NO_2 sensing characteristics of the WO_3 sensor are significantly improved by illumination as compared to that in the dark. Influences of light wavelength and light intensity on the sensing characteristics are further studied. The results show that visible light can effectively activate the WO_3 sensors and blue light is a good choice to produce room-temperature devices which are suited for NO_2 sensing applications. A sensing mechanism is proposed according to a simple adsorption–photodesorption model.

1. Introduction

Semiconductor metal oxide gas sensors are generally operated at elevated temperatures (100–400 °C) in order to accelerate chemical reactions between metal oxide surface and target gas molecules. Due to the thermo-activated chemical reactions involved in detection mechanisms of these gas sensors, working temperature is a critical parameter, as it influences sensor response, response time, selectivity, power consumption and even sensor structure. Working at a high temperature implies expensive sensor architecture, difficulties in maintaining stable sensor response and a high-power consumption. In recent years, there have been reports of gas sensors based on ultra-violet (UV) activated metal oxide semiconductors [1–3]. Illuminating these sensors with UV light is a feasible alternative to activate chemical reactions at metal oxide surface without the necessity of heating [4–6]. It was suggested that UV light affects gas sensor performance through the following ways: (1) UV light leads to dissociation of target gas and chemical surface adsorbed species [2,3]; (2) UV light increases density of free electron–hole pairs and thus facilitate carrier generation [7]. These physico-chemical phenomena allow gas sensing at room temperature and implantation of these UV activated metal oxide gas sensors in different applications, such as portable devices or low power consumption applications. Nevertheless, UV-sources are power-hungry and expensive. Compared to UV sources, visible sources are inexpensive and energy saving. Therefore, visible light is a potential candidate to substitute UV light to activate metal oxide gas sensors at room temperature.

Among metal oxides, tungsten oxide (WO_3) is a good candidate for low concentration NO_2 sensors [8–10]. WO_3 sensors usually work at a high temperature to get rapid responses. As reported in a previous work [8], WO_3 sensors prepared by atmospheric plasma spray need to be heated at about 200 °C in order to get acceptable response time and recovery time. Many techniques can be employed to deposit WO_3 sensitive layer. According to thickness of sensitive layer, manufacturing techniques can be classified in two types, i.e., thick-film process and thin-film process. The thin-film process mainly consists of physical vapor deposition and chemical vapor deposition. The thick-film process, mostly screen-printing, is well developed. A broad range of materials can be used and the cost of materials and production is relatively low. In this work, WO_3 sensitive films are prepared by screen-printing and illuminated by visible-light. In order to study the effect of light wavelength on sensing characteristics of the WO_3 sensors, the gas sensing measurements under UV-light are also performed in this work. The

* Corresponding author at: Service de Science des Matériaux, Faculté Polytechnique (FPMs), Université de Mons (UMONS), Rue de l'épargne 56, 7000 Mons, Belgium. Tel.: +32 06537 4415; fax: +32 06537 4416.
E-mail addresses: chao.zhang@umons.ac.be, zhangchao_cqu@hotmail.com (C. Zhang), marc.debliquy@umons.ac.be (M. Debliquy).

0925-4005/$ – see front matter © 2013 Elsevier B.V. All rights reserved.
http://dx.doi.org/10.1016/j.snb.2013.01.082

effects of light wavelength and light intensity on NO_2 sensing characteristics of the WO_3 sensors are investigated. The object of this work is to study the NO_2 sensing properties of WO_3 sensors under visible-light illumination at room temperature.

2. Experimental method

A commercial powder (Fluka < 100 nm) was used for deposition of WO_3 sensitive layer by screen-printing. The solvent for the paste was prepared by dissolving 0.2 g ethyl cellulose into 2.5 ml anhydrous terpineol. Three grams of WO_3 powder was mixed into 2.7 g terpineol solution. The mixture was continuously stirred for 30 min in a mechanical stirrer (Heidolph Elektro GmbH) and then submitted to a high-speed homogenizer (Kinematica AG) for 15 min until the powder was uniformly dispersed and a homogenous paste was formed. At last, the paste was screen-printed onto commercial alumina substrates equipped with Au electrodes and Pt heat element (left scheme in Fig. 1) to get 20 μm WO_3 sensitive layers. The mesh size of the screen was 160. Finally, the sensors were heated at 100 °C for 5 min and then annealed at 700 °C for 1 h to improve the mechanical bond of deposited particles so that the films would not fall off from alumina substrates.

Surface morphologies of the WO_3 powder and annealed film were observed using scanning electron microscopy (SEM, Philips XL20). Phase constitutions of the film was determined by X-ray diffraction (XRD, Siemens D5000) using a CuK_α radiation. 2θ scanning rates of $1^\circ\ min^{-1}$ for the range from 10 to 90° and $0.02^\circ\ min^{-1}$ for the range from 22.5 to 25° were used during the XRD test.

A bulb made of 20 LEDs was installed in a sealed plastic chamber, just in front of the WO_3 sensors (Fig. 1). Different bulbs with wavelengths of 380, 400, 480, 510 and 590 nm (ultra-violet, purple, blue, green and orange light) are used. The distance between the bulb and WO_3 sensors is fixed at 45 mm. Light intensity at the position of WO_3 sensor was measured by means of a photodiode (Thorlabs, FDS100).

The scheme of the gas sensing setup is given in a previous paper [11] except a modification of the test chamber. Visible-light illumination and electrical resistance measurement are performed inside the plastic chamber. The sensors were connected to a tailor-made system to get electrical resistances of the sensors. The moisture level of gas was controlled by mixing dry and wet air (by bubbling in deionized water at 25 °C) and was varied from 0 to 100%. The total gas flow rate is 1000 ml min^{-1}. When the electrical resistance of sensor was stable in air (R_{air}) and after waiting another 30 min, diluted NO_2 was introduced into the chamber. NO_2 concentrations at the outlet of the chamber were measured by NO_2/NO/NO_x analyzer. R_{NO_2} is defined when the sensor resistance is stable in NO_2. The response of gas sensor is defined as R_{NO_2}/R_{air}. In this paper, response time is defined as the time needed for the electrical resistance starting from R_{air} to reach 90% of R_{NO_2} while recovery time represents the time required for resistance decreasing from R_{NO_2} to 110% of R_{air}.

3. Results and discussion

3.1. Film microstructure

The XRD measurements were conducted on the powders and annealed films. The results in Fig. 2 show that both the powders and films presented a well-crystallized WO_3 monoclinic phase, corresponding to PDF 43-1035. In order to estimate an average grain size of the WO_3 film, a slow scan with a rate of $0.02^\circ\ min^{-1}$ was performed. The Scherrer equation with the constant K of 0.89 was utilized for the calculation. Based on FWHM values of WO_3 (0, 0, 2), (0, 2, 0) and (2, 0, 0) peaks at 23.12, 23.58 and 24.38°, the average grain size of the annealed film was around 50 nm.

The surface morphology of WO_3 powder was examined by scanning electron microscopy as shown in Fig. 3. It can be observed that the powder was agglomerated due to its small size. Fig. 4 shows the surface morphology of the annealed WO_3 films. In the films, WO_3 powders were only loosely connected with each other.

3.2. Sensing characteristics

The sensors were exposed to NO_2 under illumination with blue light. The light intensity was varied by putting red filters in front of the blue bulb. The responses to NO_2 in the dark are insignificant and response time was extremely long (Fig. 5). When the sensor was illuminated under 0.08 and 0.18 W cm^{-2} blue light, obvious improvements in response time and in particular recovery time were observed. Firstly, it can be found that the base resistance decreased with the increase of light intensity and the resistance change was a slow process, which took more than 1 h. Secondly, the sensor response, response time and recovery time were improved when the light intensity was enhanced.Fig. 6 shows electrical resistance responses of WO_3 sensor to 160 and 320 ppb NO_2 illuminated by 380–590 nm lights. First of all, it should be mentioned that the light densities were not the same for different bulbs. The light intensity was measured by a photodiode and listed in Table 1. Even if the light intensity was different, some conclusions can be drawn from Fig. 5. Firstly, the base resistance (R_{air}) decreases when a shorter wavelength light is employed. Secondly, the sensing characteristics vary with light wavelength. Sensing characteristics for different

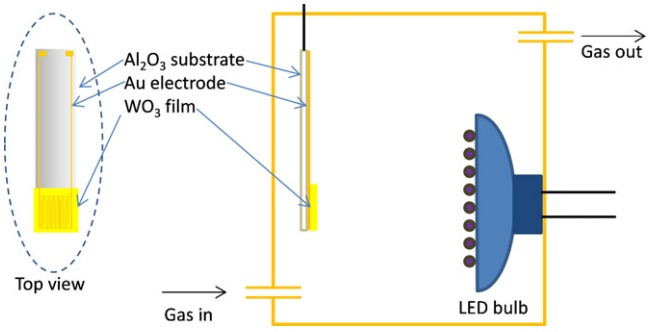

Fig. 1. Scheme of WO_3 sensor structure and test chamber.

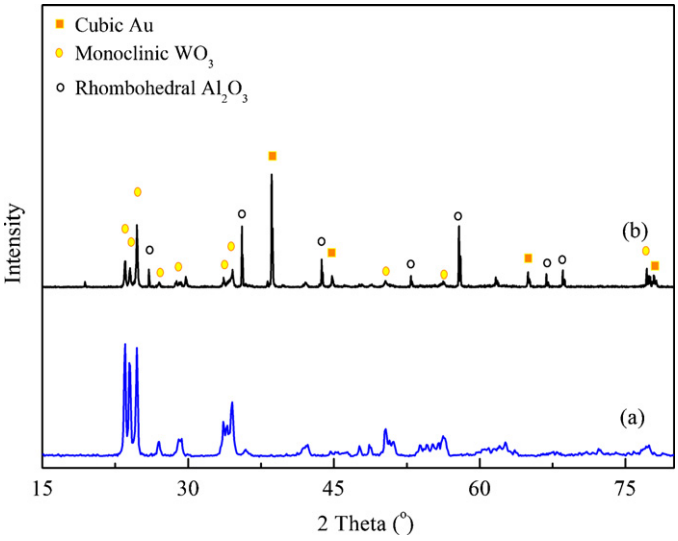

Fig. 2. XRD pattern of (a) WO_3 powder and (b) annealed WO_3 film.